JOURNAL OF GEOPHYSICAL RESEARCH, VOL. 112, C10020, doi:10.1029/2007JC004193, 2007

Longitudinal and topographic variations in North Atlantic tidal and inertial energy around latitudes 30 ± 10°N

Hans van Haren[1]

Received 28 February 2007; revised 27 June 2007; accepted 10 August 2007; published 19 October 2007.

[1] Open ocean kinetic energy is investigated at dominant inertial and semidiurnal tidal frequencies using historic current observations from the North Atlantic Ocean, around midlatitudes. Focus is on possible energy variations due to major topography changes between the eastern (Canary) and western (Hatteras, Sohm) basins, thereby crossing the Mid-Atlantic Ridge (MAR). While, in open basins on both sides of MAR, semidiurnal kinetic energy drops in magnitude by some 50% between latitudes 20°N < φ < 28°N, in agreement with TPXO-elevation data, an even larger longitudinal dependence is observed. West of MAR, semidiurnal energy is up to 30 times less than east of it. Inertial kinetic energy is either decreasing (by a factor of 2−4) westward or more or less independent of longitude. This contrasts strongly with westward intensified near-surface inertial energy fluxes previously found. The latter fluxes also did not show an increase (by a factor of 5−10) for 25°N < φ < 30°N as observed here for inertial energy in both basins. West of MAR, the internal wave background level for frequencies up to sixth diurnal is much less, by a factor of 3−10, at tidal-inertial interaction frequencies than east of MAR. No significant atmospheric or large-scale vorticity influence, or seasonal variations therein, is found on inertial energy content across the basin. As no individual peaks are observed at frequencies K_1, O_1 and M_1, S_1, direct diurnal tidal forcing and subharmonic resonance must be accompanied by nonlinear interactions in possibly enhancing inertial energy at the critical diurnal latitude.

Citation: van Haren, H. (2007), Longitudinal and topographic variations in North Atlantic tidal and inertial energy around latitudes 30 ± 10°N, *J. Geophys. Res.*, *112*, C10020, doi:10.1029/2007JC004193.

1. Introduction

[2] Motions in the deep ocean are dominated at a limited set of periodicities or frequencies: 'large-scale' subinertial motions, which have periods of a day and longer, inertial motions, due to the rotation of the Earth, and tidal motions. Although these motions dominate nearly everywhere in the ocean, their relative contribution varies considerably from place to place. In a few exceptional areas one or more of them may even become negligible, such as tides in parts of the Mediterranean Sea [*Perkins*, 1972] and inertial motions in the Faeroe-Shetland Channel [*Hosegood and van Haren*, 2006]. However, also in the open ocean horizontal spatial variations may result in differences larger than one decade in kinetic energy (E_k) at a particular frequency. In the vertical, one decade variations in E_k can be attributed to variations in buoyancy frequency N, which is proportional to the vertical density stratification, but such variations are not the subject here.

[3] The aim of the present study is to evaluate horizontal spatial variations in inertial and semidiurnal tidal kinetic energy using historic current observations and to infer possible relationships with topographic and latitudinal variations. These frequency bands partially contain motions that are highly coherent in the vertical, such as barotropic tidal currents driven by the tidal potential, and they partially contain incoherent motions that have short O(100 m) vertical scales, including 'intermittent' (inertial) internal waves driven by baroclinic pressure gradients in the ocean interior. The data to be analyzed are from midlatitudes in the North Atlantic Ocean, which is the most densely sampled ocean area using moored current meters (Figure 1). At these latitudes the internal wave band contains at least semidiurnal tidal frequencies, as it is defined between frequencies f < σ < N, for N ≫ f, f = 2Ωsinφ represents the inertial frequency, the vertical component of the Earth's rotational vector $\mathbf{\Omega}$ at latitude φ.

[4] The western part of the present area of investigation has been extensively studied using observations for its variations in tidal [*Wunsch*, 1975] and inertial kinetic energy [*Fu*, 1981]. Fu pointed out that above abyssal plains the entire E_k spectrum is fairly smooth except for peaks at f and, smaller in height, at semidiurnal lunar M_2. In contrast, above 'rough topography', the Mid-Atlantic Ridge (MAR) extensions, the spectrum was less smooth including peaks at (not named) higher harmonics. According to Fu, the inertial peak height (defined with respect to the spectral 'background') was larger by about a decade above rough topo-

[1]Royal Netherlands Institute for Sea Research (NIOZ), Den Burg, Netherlands.

0148-0227/07/2007JC004193$09.00

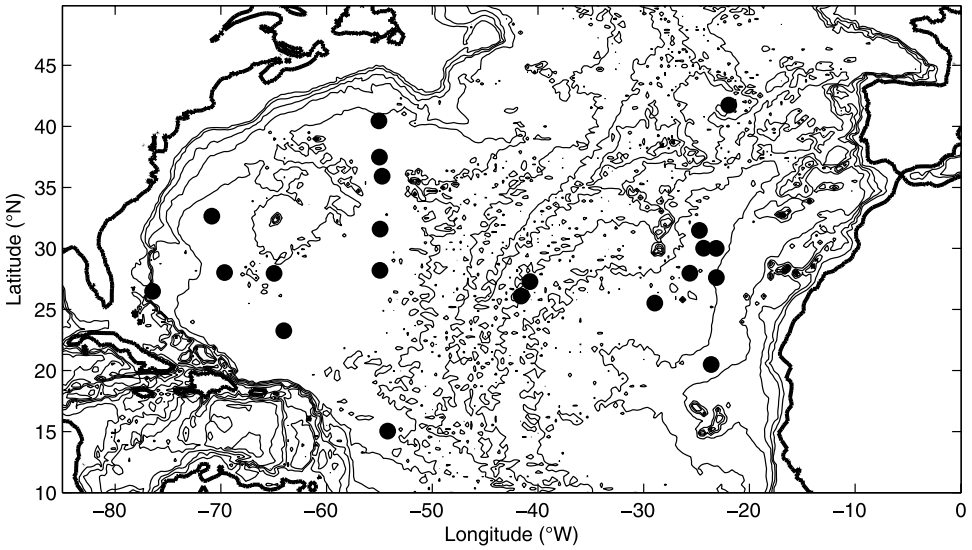

Figure 1. North Atlantic Ocean moored current meter sites (black dots) of which data are used in this paper.

graphy compared to that above smooth topography. It was noted that while the latter E_k data WKB-scaled with N, the former did not. *Fu* [1981] neither gave an explanation for the observed lack of WKB scaling in MAR data, nor for the increased energy at tidal (higher) harmonics in these data, but he did attribute the apparent enhancement of inertial energy to local topographic effects.

[5] As for spatial variations at tidal frequencies, recent global-scale observations and modeling [*Morozov*, 1995; *Egbert and Ray*, 2001; *Simmons et al.*, 2004] suggest a topographic-longitudinal (λ) variation of baroclinic semidiurnal (henceforth 'D_2' when no specific harmonic constituent is meant) tidal energy, its flux and its dissipation. Specifically, in the North Atlantic Ocean, E_k(baroclinic D_2) enhancement is indicated, albeit not exclusively, near major topography, including continental slopes and MAR, and in the eastern Azores-Canary basin. Others suggest an eastward intensification of (barotropic) tidal elevation as inferred from TPXO [*Egbert et al.*, 1994]. The same data suggest a relative minimum in a band between $20°N < \varphi < 25°N$. In addition, modeling results and observations demonstrate a latitudinal variation in (baroclinic) semidiurnal tidal (and inertial) energy [*Nagasawa et al.*, 2000; *Hibiya et al.*, 2002; *MacKinnon and Winters*, 2005; *van Haren*, 2005], which are suggested (partially) due to subharmonic resonance resulting in enhanced E_k(f) and decreased $E_k(D_2)$ near $|\varphi| \approx 29°$. Earlier observations of short length, between $\sim$1 and 15 days, already indicated an amplitude increase by a factor of about 2 at half a degree equatorward of the S_1 (half S_2) = f 'critical latitude' with respect to other latitudes [*Ekman*, 1953; *Reid*, 1962; *Hendershott*, 1973]. Half M_2 remained uninvestigated. While *Ekman* [1953] demonstrated deeper phase variations in North Atlantic inertial motions, the latter two authors considered only surface motions, from the North Pacific. They suggested that the locally enhanced E_k(f) was directly driven by the diurnal tide, propagating exclusively equatorward under the traditional approximation. Using half-year-long east Atlantic time series, *van Haren* [2005] pointed out that no evidence was found there for peak enhancement at harmonic diurnal tidal frequencies.

[6] The locally increased E_k(f) near this critical latitude, where $f \approx D_1$, may also be (partially) due to favorable atmospheric near-surface stratification conditions, resulting in the ubiquitous geostrophic adjustment of transients [*Millot and Crépon*, 1981] or direct slab-layer generation [*Pollard and Millard*, 1970]. If important, a seasonal dependence is expected with increased atmospheric disturbances in winter (favoring f-motions' generation) and near-surface mixing (weakening f-generation upon increasing the thickness of the homogeneous near-surface layer). Also, slightly more to the north between $30°N < \varphi < 45°N$, *Watanabe and Hibiya* [2002] and *Alford* [2003] predict westward intensified near-surface fluxes to inertial motions generated via slab-layer modeling.

[7] The continued investigation of temporal and spatial variations in inertial-tidal baroclinic energy is motivated in part because of its importance for deep-ocean mixing, as motions at these frequencies induce the largest shear that may lead to breaking of short-scale internal waves and subsequent irreversible mixing.

2. Data and Methods

[8] The OSU deep-water archive is the main supplier of the moored current meter data analyzed here. These are supplemented with some historic [*Siedler and Paul*, 1991] and recent data from the Canary Basin and with historic data from the WHOI current meter archive. Focus is on midlatitudes in the North Atlantic Ocean (Figure 1 and Table 1).

[9] The data search is made using the following criteria: sampling rate at least once per 2 hours, water depth $\geq$4000 m, away from large topography except for MAR, sites between latitudes $15°N < \varphi < 40°N$, instruments well away (>500 m, >50 m) from surface and bottom boundary layers, respectively. Relatively few data are from 'rough topography' area MAR, unfortunately. Preferably, data are

Table 1. Moored Current Meter Data Between 15°N and 40°N, Primarily Along About −23° and −55°W (North Atlantic Ocean)[a]

Position N	Position W	Length, Start,[b] Days, Date	H, m	'1500' m |z|, m	'4000' m |z|, m
41°44.9′	21°57′	370, 10/10/1980	3840	1500	3800
31°28.8′	24°43.8′	308, 20/11/1985	5444	1016	4368
30°00.1′	*23°08.3′*	*530, 16/03/2003*	*5137*	*1550*	*3850*
		540, 22/10/2004			
30°01.4′	24°20′	240, 08/11/1987	5300	1000	5175
27°58.4′	25°38′	220, 09/11/1987	5250	1130	5190
27°36.8′	*23°07.8′*	*540, 23/10/2004*	*4930*	*1450*	*3550*
25°31.9′	28°57.2′	240, 15/10/1992	5700	1500	3500
20°29.6′	23°37′	370, 13/11/1986	4540	1255	4505
40°27.1′	55°03′	270, 11/10/1976	5173	-	4000
37°29.3′	55°00′	260, 13/10/1976	5334	1500	4000
35°55.3′	54°44.4′	230, 05/10/1976	5318	1500	4000
31°35.2′	54°56.0′	300, 16/12/1975	5587	1500	4000
28°12.6′	54°56.6′	260, 05/08/1974	5600	1000	4000
23°15.1′	64°02.1′	345, 23/11/1985	5846	1450	2900
15°02.1′	54°12.9′	350, 12/05/1977	5240	2540	4000
27°17.5′	40°45.4′	340, 12/06/1977	4360	1500	-
26°06.0′	41°36′	345, 14/06/1977	4300	-	4000
27°57.6′	64°57.8′	270, 29/07/1974	5363	1000	4000
28°01.4′	69°38.9′	210, 26/07/1974	5462	1500	4000
32°38.6′	70°50.7′	300, 16/09/1980	5410	1060	4060
26°29.3′	*76°26.9′*	*550, 06/10/1988*	*4850*	*1200*	*3800*

[a]H represents the water depth and |z| represents instrument depths that are grouped in two depth categories. Data from italicized positions are used for (monthly) time series analysis.

[b]Of each mooring, the shortest length is indicated. Dates are given as dd/mm/yyyy.

compared from the same depth levels, but this had to be changed to the same depth ranges (=depth level ±250−500 m), as few moorings resolved the entire water column well. Also, the initial criterion of at least 1-year length of time series could not be maintained. It was changed to >7 months length. For the Canary Basin (eastern North Atlantic Ocean, EAO) this posed not a big problem, as all moorings were deployed in the fall, so that a seasonally consistent data set was obtained. For the other (mainly Western North Atlantic Ocean, WAO) data no such compromise could be obtained. However, as will be demonstrated in section 3.1, the seasonal variation in kinetic energy of the internal wave band is at best ambiguous and no systematic error is observed in using 7 months mean data from instruments starting at an arbitrary date in a particular year. Naturally, only a few data sets are obtained in any particular year of deployment. It is a priori assumed that this does not hamper the present analysis.

[10] Data are not selected on current meter type, most of them are mechanical Aanderaa RCM5, 7 or 8, with a few VACM and Geodyne. Only recent Canary Basin data are obtained using acoustical RCM11 and RDI-ADCP (acoustic Doppler current profiler). It is noted that the accuracy of acoustical instrumentation is less (by a factor of 3−10 in current speed) than that of mechanical devices as inferred from the Nyquist values (Figure 2). As a result, the high-frequency internal wave band is generally not well resolved by acoustical instruments. On the other hand, their performance is more robust as they do not rely on mechanical operation, although they do need sufficient scatterers for a reasonable signal-to-noise ratio. The example comparison between data from acoustical and mechanical current meters in the same moorings in Figure 2 shows that both resolve equally well the 'low-frequency internal wave band' motions like at f and D_2, at least beyond the fourth diurnal band. No corrections have been applied to the records other than those (unknown) applied before data banking. This includes no corrections for mooring motions that were occasionally large in surface-bottom moorings [*Siedler and Paul*, 1991], but negligibly small in a recent deep subsurface mooring (e.g., <2 m vertically for a 3700-m-long Canary Basin mooring).

[11] The internal wave kinetic energy is not scaled using the buoyancy frequency N. Such scaling may be applicable for small-scale tidal energy, but less clearly for large-scale tidal energy, as 'low modes' encompass the entire water column across scales larger than the buoyancy scale. It may also be less clearly applicable for near-inertial energy, which may even increase at larger depths, smaller N (see Figures 2 and 3). Furthermore, precise N(x, y, z, t) are unknown over

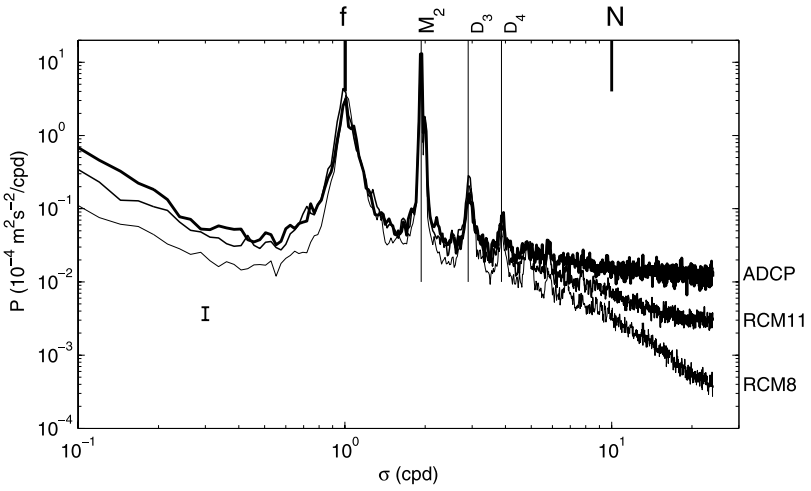

Figure 2. Spectral comparison of 1.5 years of Canary Basin data in a single mooring for acoustic devices (RDI-75 kHz ADCP, 1140 m, thick line; Aanderaa RCM11, 1460 m, medium line) with a mechanical Aanderaa RCM8 (2260 m, thin line).

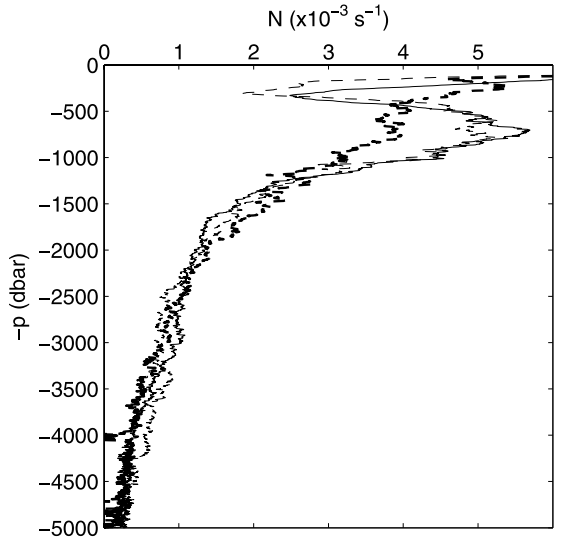

Figure 3. Buoyancy frequency profiles computed from CTD data using vertical scale $\Delta z = 100$ m and obtained in different summers at different longitudes at ∼28.9°N (all deeper than 5000 m): −24.2°W (thin solid line; Canary Basin, August 1988), −52.3°W (thin dashed line; just west of MAR, July 1997), and −66.0°W (thick dashed line; southwest of Bermuda, August 1997).

each period of deployment and around each mooring site. Therefore data are grouped in two depth ranges (1000−1500 m and ∼3500−4500 m) across which mean N varies by less than a factor of 2 (Figure 3 and Table 1).

[12] Although between WAO and EAO basins substantial variability is seen in the upper ∼1000 m of vertical profiles of N obtained in different years, with larger near-surface summer stratification and larger N around ∼700 m due to Mediterranean outflow in EAO, N profiles are relatively similar to within ∼20% for depths greater than 1100 m. As a result, (scaling) differences in E_k are not expected from vertical density stratification, when observed at the same depth levels at different φ, λ.

[13] E_k densities are determined for four frequency bands by summing the spectral contents of the band with $\sigma <$ 0.3 cpd (1 cycle per day = $2\pi/86400$ s^{-1}), the f-band, the D_2-band, and the band between $3 < \sigma < 6$ cpd. The latter contains moderately high-frequency internal waves including some inertial-tidal higher harmonics. For capturing >90% of the energy in the f- and D_2-bands, one requires a mean relative bandwidth $\Delta\sigma/\sigma = 0.09$, as observed in Bay of Biscay and Canary Basin data [*van Haren*, 2004a]. In practice, a band-pass filter $0.96M_2 < \sigma < 1.05M_2$ is used for D_2, but a 2 times wider band $0.9f < \sigma < 1.1f$ is used here, because the f-band peak frequency wanders about 5% around the canonical 1.02f. The peak frequency needs to be established before the 9% band borders can be established. Using the wider band with fixed border frequencies avoids the, often manual, search for the precise peak frequency, which can be ambiguous as the f-band is generally fairly flat. As little energy (<10%) is found outside the band around the f-peak this ensures the same result, to within a small 'error', as using the 0.09 relative bandwidth filter, as has been tested, and used previously [*van Haren*, 2005], for Canary Basin data. The above summing of spectral contents for 7 months time series yields energy estimates to within a relative error of ∼12%.

3. Observations

[14] Two example spectra show a distinct difference between deep basins in WAO and EAO (Figure 4). In EAO, semidiurnal tides dominate above subpeaks at f and inertial-tidal harmonics, while in WAO the low-frequency (Gulf Stream extension) motions dominate over the relatively featureless internal wave band. This featureless internal wave band, with a relatively small M_2 peak, resembles best the canonical GM internal wave spectrum [*Garrett and Munk*, 1972]. This is surely not the case for EAO, although it adopts the canonical σ^{-2} slope when smoothed heavily. In this example, f is about equally energetic in both basins while tidal (harmonics) energy is some 20 times larger in EAO than in WAO. Only at non-'deterministic', internal wave band 'background' frequencies between tidal harmonics and inertial-tidal interaction frequencies, especially between $f \ll \sigma \ll M_2$, energy in WAO is comparable to that in EAO. Below, details of latitudinal and longitudinal variations in different energy bands will be investigated. First however, possible effects of seasonal variations are investigated, as some WAO data sets are not covering the same late autumn-winter-spring period as the EAO data.

3.1. Seasonal Variability

[15] In general, inertio-gravity waves depend in amplitude and propagation direction largely on 'background' reduced gravity, when N > f. Any variations in N may thus result in variations in internal wave kinetic energy E_k(IW). Spatial, especially horizontal, variations N(x, y) are of some interest in the present study. However, in order to evaluate their effects significantly one needs to address potential bias by temporal variations N(t) that have timescales comparable to the length of time over which E_k is computed, typically a month or longer. This is because typical time series' lengths are 7 months with arbitrary starting date (except in EAO), which should be contrasted with the possible effects of seasonal variations in N.

[16] Such seasonal variations in N are certainly large in the upper 100 m of the ocean, but it is not precisely known how this affects the interior N(t, |z| > 100 m). Directly, deep N are not affected by seasonal effects except in areas of deep-water formation. As for the supported internal waves, dominant near-surface inertial waves are commonly thought to be generated following geostrophic adjustment or direct slab-layer generation after the passage of atmospheric disturbances, which show a seasonal variation. However, in slab-layer generation the amplitude of inertial motions also heavily depends on the thickness of the homogeneous near-surface layer and the value of N below [*Pollard and Millard*, 1970]. Thus, although wintertime storms may be energetic, the deepening of the near-surface mixed layer and associated reduction of N may not always lead to larger E_k(f) in the interior.

[17] To verify seasonal variability in E_k, several at least year-long time series are divided in monthly records of which the inertial and tidal spectral contents are determined to within a spectral resolution of 0.05 cpd. To investigate to occurrence of a seasonal cycle in these data, winter is

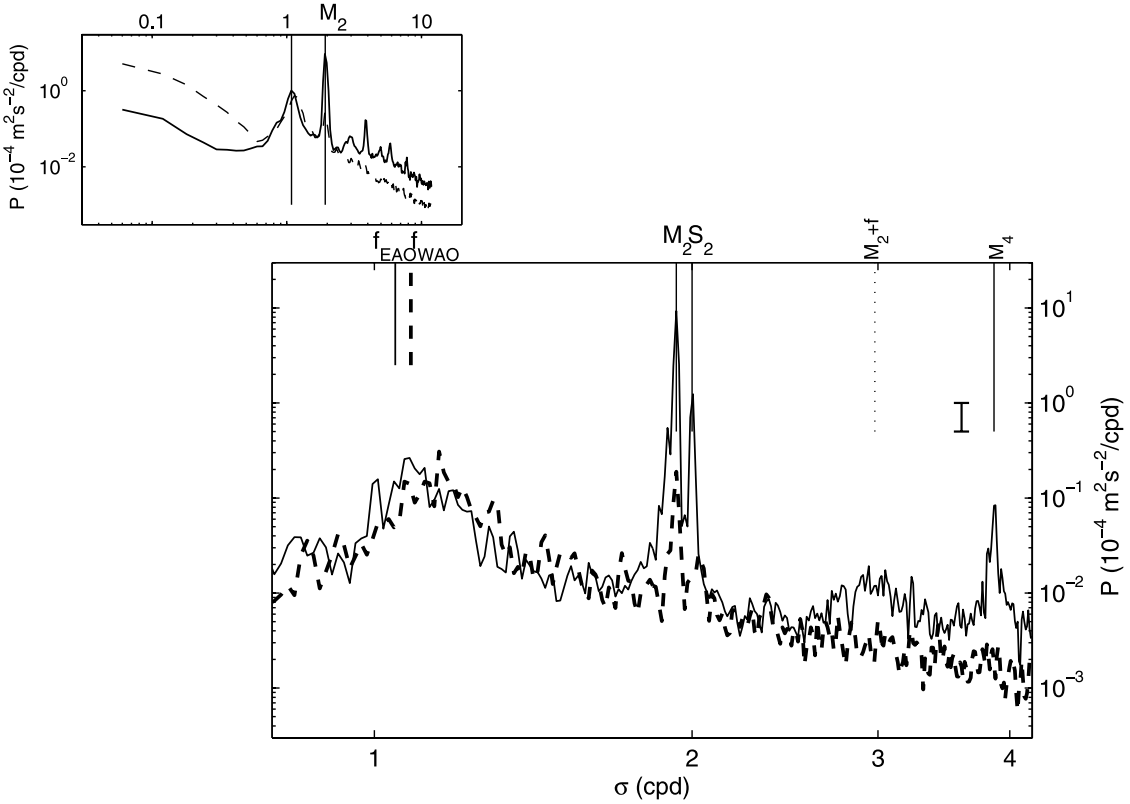

Figure 4. (top left) Smoothed overview and (bottom right) moderately smoothed detail example of kinetic energy spectra comparing 310 days' records of Aanderaa RCM-5 current meter data from the eastern North Atlantic (thin solid line) and from the western North Atlantic Ocean (thick dashed line). Both data sets are from open ocean basins, at ~4000 m (H ≈ 5400 m): at 32.8°N, −70.8°W obtained in 1981/1982, and at 31.5°N, −24.4°W in 1985/1986.

defined following the meteorological definition: including the months of December, January and February (for the Northern Hemisphere), while a 'summer mean' implies averaging over data from the months of June, July and August. At a depth of ~1500 m some series significantly show a seasonal cycle, but in $E_k(f)$ only (Figure 5). A seasonal cycle is not found significantly (to within a relative error of ~30%) in many other $E_k(f)$ series and not in any $E_k(D_2)$ at 1500 m, and also never deeper down (~4000 m) at either f or D_2.

[18] In the $E_k(f)|_{1500}$ record with a significant seasonal signal (Figure 5d), individual energy levels may vary by a factor of up to 8 through the record, but seasonal (winter, summer) means differ by utmost a factor of 2. As a result, averaging over 7 months with arbitrary starting date will yield a maximum relative error of 30%, about 2.5 times the noise error of ~12% and much less than spatial variations to be observed below.

[19] Note that such variability as found in (Figure 5d) is also found in the monthly time series of D_2 or in other series of f, albeit appearing quasirandomly (e.g., Figures 5b, 5c, and 5e). For reference, a similar, relatively large magnitude of monthly variations is found in pressure and temperature data for D_2 (Figure 5a). Especially pressure spectra show a large peaking dominance of tidal constituents, which, however, are apparently strongly modulated. These are partially due to long-term modulations in tidal constituents, but also due to variations in internal waves modulated by background conditions, as suggested for the incoherent part in tide-gauge records showing similar spectra [*Colosi and Munk*, 2006]. Although it is unknown whether the monthly variations in $E_k(f)$ are likewise caused by local variations in N or by low-frequency vorticity ζ, it seems that they are generally fairly independent of season and horizontal position, for the present data: no clear seasonal (annual) cycle is observed in E_k, and thus 7-month time series with arbitrary starting date can be compared with each other in the analysis below.

3.2. Latitudinal Variations in 7-Month Mean E_k

[20] Computing average kinetic energy in the bands f and D_2 for data from EAO between October and May [*van Haren*, 2005] observed a peak enhancement in $E_k(f)$ by a factor of 9 (6) at ~1500 m (~4000 m) for $\varphi \approx 28°$N with respect to $|\varphi| < 25°$ and $\varphi > 31°$N. Some of these results are repeated here for comparison in graphical form (part of Figure 6), to which are added subinertial (sf) and moderate internal wave band (mIW) energy variations with latitude. In the open WAO basin (Figure 6, left), very similar observations are made despite a possibly larger relative error of maximum 30% due to varying winter-summer contributions: $E_k(f)$ peaks near $\varphi \approx 28°$N, by a factor of 6 at both depth levels compared to other latitudes. This is also obvious in the individual spectra (Figure 7) from which

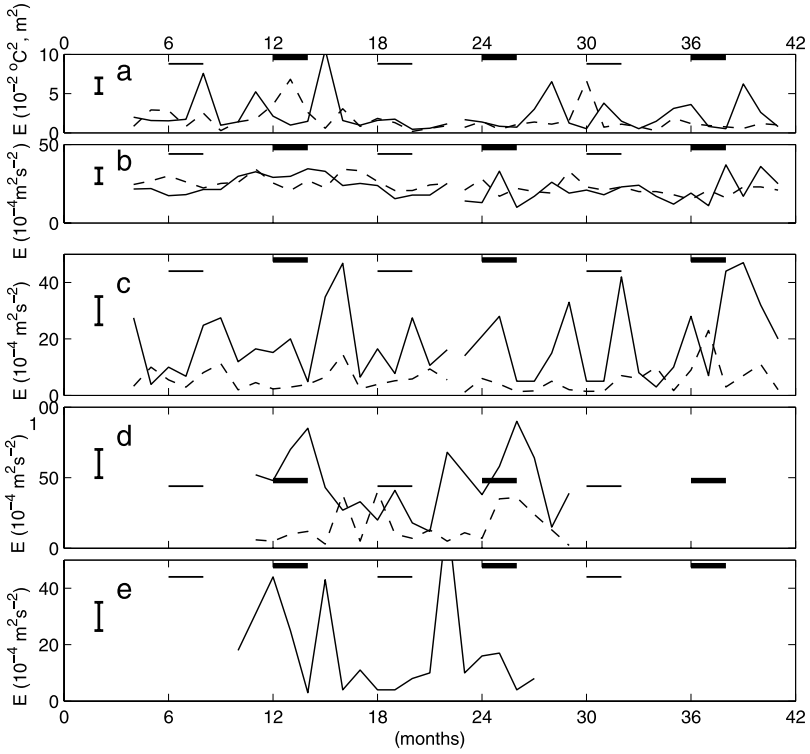

Figure 5. Time series (in months following a starting month in a particular year, with the following years +12, +24, +36) of 30 days averaged spectral contents for (Figures 5b–5e) $|z| \sim 1500$ m (solid lines) and $|z| \sim 4000$ m (dashed lines). Winter periods (thick bars) are months 12–14, etcetera, summer (light lines) months 6–8, etc. (a) Integrated spectral densities for pressure (solid) and temperature ($\times 100$, dashed) at 1450 m, 30°N, −23°W EAO starting March 2003. (b) $E_k(D_2)$ at 30°N, −23°W EAO, starting March 2003. (c) Corresponding $E_k(f)$. (d) $E_k(f)$ at 27.6°N, −23°W EAO, starting October 2004. Note the different vertical scale. (e) $E_k(f)$ at 26°N, −76°W WAO, starting October 1988.

these band averages are computed. Like in the EAO spectra [*van Haren*, 2005], individual peaks at diurnal tidal frequencies O_1, K_1 and subharmonic half M_2, half S_2 (M_1, S_1) are not observed significantly different from their spectral surroundings; they are part of a relatively broad f-band (Figure 7).

[21] Especially the ter-diurnal band varies in magnitude with the near-inertial band, which together with larger variance at surrounding frequencies causes E_k(mIW) to mimic $E_k(f)$ at 1500 m in WAO (Figure 6). A major difference between WAO compared to EAO occurs for $\varphi > 35$°N, where, especially at 1500 m, $E_k(f)$ and E_k(mIW) relatively increase. This is associated with an increase in E_k(sf), presumably because of the Gulf Stream and its eddies. This increase at the WAO side is also visible in near-surface inertial wave fluxes (Figure 6). However, these fluxes do not show the critical diurnal latitude increase (between 25°N and 30°N), which is thus presumably not locally generated from atmospheric disturbances. Rather independent of φ, both $E_k(f)$ [and E_k(mIW)] differ by a factor of 3 between ∼1500 and ∼4000 m, which is slightly less than the factor of 4 estimated in N variation between these depths (Figure 3). Note that no consistent depth variation is found for $E_k(D_2)$ and, variably, in E_k(sf). At some latitudes $E_k(D_2)$ is larger at greater depths compared to 1500 m.

[22] In latitudinal direction in both EAO and WAO, $E_k(D_2)$ is found significantly (to within a relative error of 12%) reduced by ∼50% near $\varphi \approx 25$°N with respect to other latitudes. A similar dip is visible in the TPXO surface elevation (generation), although slightly more equatorward by ∼3°. In contrast with EAO data, $E_k(D_2)$ in WAO seems persistently weaker at 4000 m compared to 1500 m, but only by a factor of ∼1.5–2 compared to the factor of 3 again observed for $E_k(f)$ and E_k(mIW) between these depth levels.

[23] Another difference between WAO and EAO concerns the amplitude of a given band at a particular latitude. While the latitudinal variations are consistent between the two basins, the amplitudes are generally, but not always, less in WAO compared to EAO, except, of course, for $\varphi >$ 35°N.

3.3. Longitudinal Variations in 7-Month Mean E_k

[24] Along a particular latitude across the North Atlantic Ocean, observed $E_k(f)$, $E_k(D_2)$ and E_k(mIW) decrease nearly monotonically from east to west (Figures 8 and 9), while E_k(sf) remains constant until the western boundary (Gulf Stream) is reached (not shown). The main discrepancy in the monotonic east–west decrease is MAR, above which D_2 energy increases at 1500 m along with, marginally significant, E_k(mIW) and $E_k(f)|_{1500}$, but with a decrease in

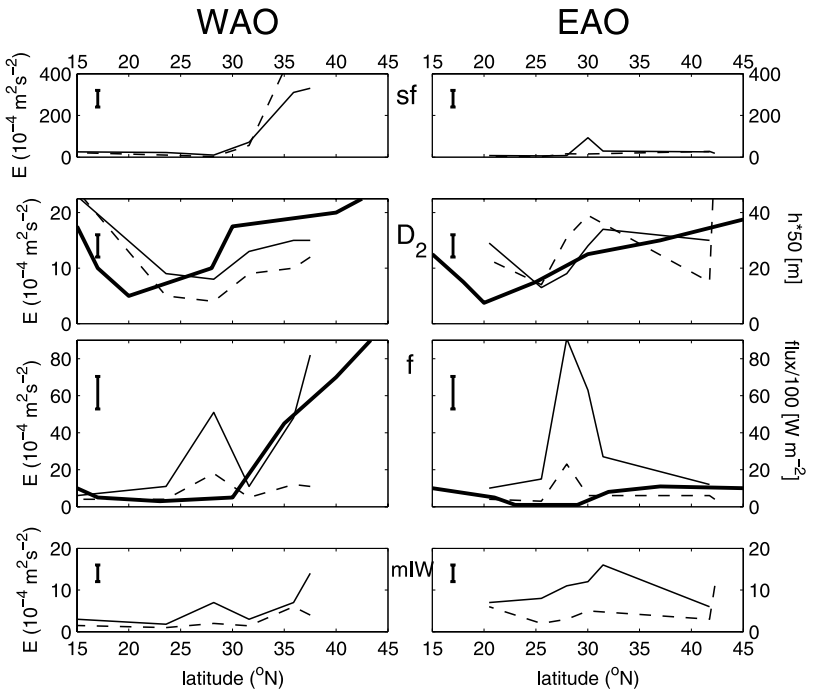

Figure 6. Latitudinal variation of 7 months mean kinetic energy at depth levels ~1500 m (solid lines) and ~4000 m (dashed lines) in (left) WAO (along ~−55°W) and (right) EAO (along ~−23°W) for the frequency bands: subinertial (sf) $\sigma < 0.2$ cpd, semidiurnal tidal (D_2) $0.955M_2 < \sigma < 1.055M_2$, inertial (f) $0.9f < \sigma < 1.1f$, and moderate internal wave band (mIW) $3 < \sigma < 6$ cpd. Note the different vertical scales for the different bands and, for D_2, for the different longitudes. The thick solid lines in the D_2 panels are surface elevation (×50 m) taken from the TPXO model by *Egbert et al.* [1994]. Similar lines in the f panels represent surface inertial wave fluxes (/100 W m^{-2}) taken from *Alford* [2003].

$E_k(f)|_{4000}$. As in the latitudinal variations, mIW is dominated at D_3 and D_4, which show as peaks in EAO, but blend in the smooth sloping background in WAO. Also, values in $E_k(f)$ and $E_k(mIW)$ observed at ~1500 m differ by a factor of ~3 with those observed at ~4000 m, nearly independent of longitude. Again, $E_k(D_2)$ is more constant with depth implying that it is more than $E_k(f)$ dominated by large-scale coherent tidal motions. However, such motions are never-

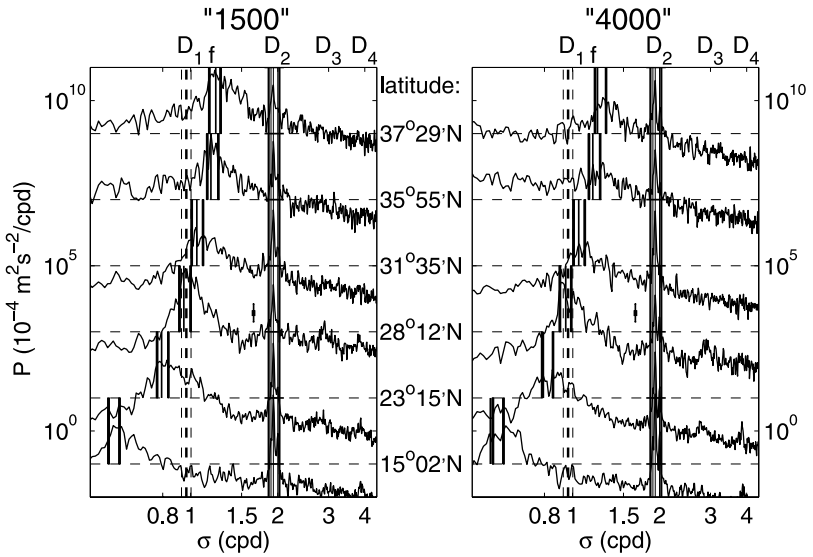

Figure 7. Internal wave band spectra for 7 months of WAO observations along ~−55°W for (left) ~1500 m and (right) ~4000 m. Per latitude, spectra are offset by 2 decades in the vertical. Two decades is also the height of the inertial band between the thick bars around its local frequency, and here indicating the same relative width $\Delta\sigma/\sigma = 0.09$ as for the semidiurnal band.

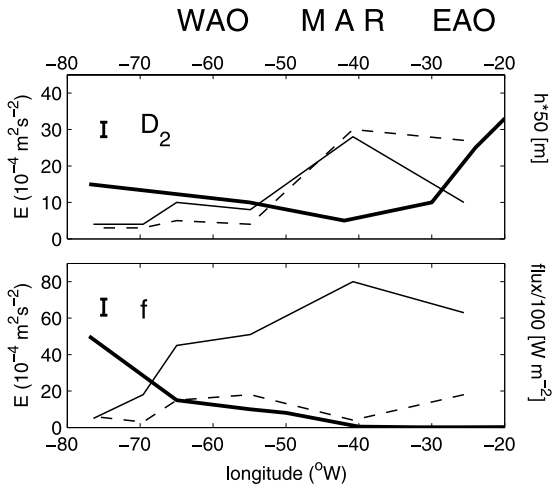

Figure 8. Same as Figure 6 ($E_k(f)$ and $E_k(D_2)$ only) for longitudinal variations at $\varphi \approx 28°N$, the latitude where relatively large inertial kinetic energy is observed in both WAO and EAO. Note the different vertical scales.

theless at least somewhat affected by large-scale topography, as the TPXO elevation model data do show an eastward increase but not at MAR [*Egbert et al.*, 1994]. The eventual decrease between EAO and WAO amounts (at $\varphi \approx 28°N$): a factor of 7 for $E_k(D_2)$, a factor of 4 for $E_k(f)|_{1500}$ and a factor of 2 for $E_k(f)|_{4000}$. The latter two contrast with a westward intensification of near-surface inertial wave flux [*Watanabe and Hibiya*, 2002; *Alford*, 2003]. At other latitudes, similar longitudinal variations are found, although they may vary by a factor of 2 compared to these values (see Figure 4, where the deep inertial energy barely changes with longitude).

4. Discussion

[25] Spatial variations in midlatitude North Atlantic Ocean kinetic energy seem less dominated by rough topographic effects than previously assumed. Compared with the abyssal, open Canary Basin the Mid-Atlantic Ridge only marginally shows enhanced tidal and inertial energy, and even decreased levels of near-bottom inertial energy. Note that, limited, current measurements above MAR were well outside the reflective zone of topography at 300 m above the bottom. This questions the importance of local versus remote internal tide generation. It also questions the influence of rough topography on (internal wave induced) open-ocean mixing. Some evidence suggests that above abyssal plains near-inertial energy is enhanced outside the bottom boundary layer, >50 m above the bottom [*van Haren*, 2004b], and that the eddy diffusivity may be well exceeding the canonical value of 10^{-4} m^2s^{-1}, just like above topography as MAR [*Walter et al.*, 2005]. It is noted however, that the turbulent fluxes are relatively low above abyssal plains, owing to weak stratification in general.

[26] Following basin-scale ocean modeling [*Egbert and Ray*, 2001; *Simmons et al.*, 2004], large-scale topographic sites in the North Atlantic Ocean show enhanced internal tidal energy flux and dissipation, but in the EAO mainly. In the results from these models the distinct topography of MAR is not very well visible. This confirms the present inferences, although more dedicated data are wanted. In the above models, also a local minimum in tidal flux and dissipation seems to occur between $20° < \varphi < 25°N$, but especially only in EAO and a clear band in latitudinal direction is not seen. Such a band is seen in the minimum TPXO tidal elevation at more or less similar latitudes.

[27] As for a possible relation between $E_k(D_2)$ and $E_k(f)$ a definite answer has to be found yet. Most extensive inertial wave generation near the surface seems to occur in WAO, as that area sees the passage of most intense tropical cyclones. There, also the largest subinertial (wind-driven boundary) current exists, the Gulf Stream. However, none seems to affect $E_k(f)$ in the interior ocean, as the inertial energy is not larger in WAO than in EAO, except poleward of 35°N. As in both WAO and EAO, as well as in the Pacific [*Hendershott*, 1973], $E_k(f)$ peaks in latitudinal direction around $\varphi \approx 28°N-30°N$, subharmonic resonance

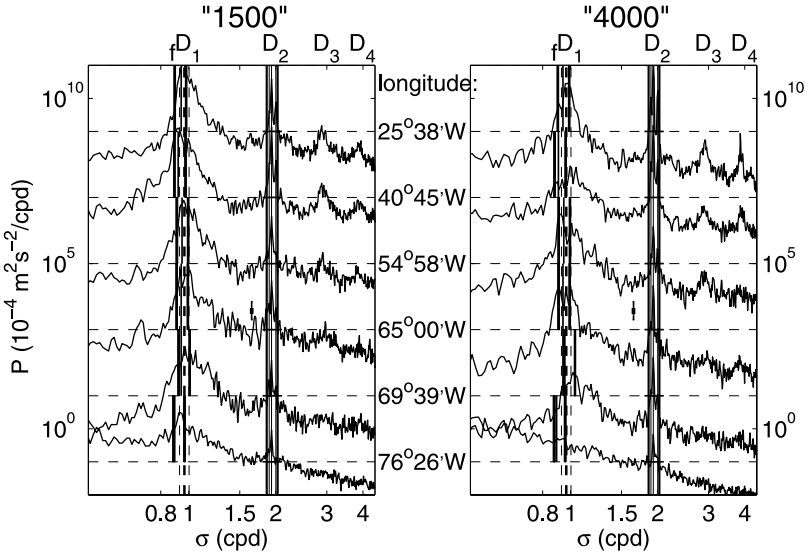

Figure 9. Same as Figure 7, but for the sites in Figure 8.

(SR) from $D_2 \rightarrow D_1 \approx f$ seems an important mechanism for generating short-scale motions. Favorable local conditions may also be the near-surface stratification conditions, but not in such a narrow latitudinal band.

[28] However, the problem with positively identifying the evidence for SR in these data is that harmonic frequencies like M_1 and S_1 do not show as distinct peaks, but as finitely broad bands incorporated in the f-band, while short-scale inertial motions are also found poleward from this area, albeit having smaller amplitudes. As a result, one (or more) secondary interaction mechanisms must be at work besides SR, which govern the familiar spectral broadening of the inertial band, also at the critical latitude. Similarly, direct diurnal (tidal) forcing suggested by *Reid* [1962] and *Hendershott* [1973] seems not uniquely important, as peaks at K_1 and O_1 are not observed, besides a resonance interaction mechanism being unknown.

[29] Such an interaction governing a band broadening also leads to higher harmonics as modeled by *Xing and Davies* [2002]. This redistributes energy to smaller internal wave scales, possibly eventually leading to wave breaking and mixing. Both f and D_2 seem the major contributors to these higher harmonic interaction frequencies, so that their combination seems prominent. In contrast, the much smoother spectral shapes in WAO sometimes show elevated levels compared to EAO data at intermediate frequencies, suggesting a more random internal wavefield in an area where at least one contributor (the tide here) is weak, just like in the Mediterranean Sea.

[30] **Acknowledgments.** Margriet Hiehle made Figure 1. I thank Gerold Siedler for the use of some IfM Kiel Canary Basin data. I also thank Charmaine King and Carl Wunsch for the expedient response following my request to use some WHOI current meter archive data. The recent Canary Basin data are acquired with funding from the Netherlands Organization for the Advancement of Scientific Research (NWO) during project "LOCO." All other data are from the deep-water archive maintained by the Buoygroup of Oregon State University (OSU), Corvallis, Oregon. The comments by two anonymous referees were very helpful in improving an earlier draft of this paper.

References

Alford, M. (2003), Improved global maps and 54-year history of wind-work on ocean inertial motions, *Geophys. Res. Lett.*, *30*(8), 1424, doi:10.1029/2002GL016614.

Colosi, J. A., and W. Munk (2006), Tales of the venerable Honolulu tide gauge, *J. Phys. Oceanogr.*, *36*, 967–996.

Egbert, G. D., and R. D. Ray (2001), Estimates of M_2 tidal energy dissipation from TOPEX/POSEIDON altimeter data, *J. Geophys. Res.*, *106*, 22,475–22,502.

Egbert, G. D., A. F. Bennett, and M. G. G. Foreman (1994), TOPEX/POSEIDON tides estimated using a global inverse model, *J. Geophys. Res.*, *99*, 24,821–24,852.

Ekman, V. W. (1953), Studies on ocean currents: Results of a cruise on board the Armauer Hansen under the leadership of Björn Helland-Hansen, *Geofys. Publ. 19-1*, 228 pp., Norw. Acad. of Sci. and Lett., Oslo.

Fu, L.-L. (1981), Observations and models of inertial waves in the deep ocean, *Rev. Geophys.*, *19*, 141–170.

Garrett, C. J. R., and W. H. Munk (1972), Space-time scales of internal waves, *Geophys. Fluid Dyn.*, *3*, 225–264.

Hendershott, M. C. (1973), Inertial oscillations of tidal period, *Prog. Oceanogr.*, *6*, 1–27.

Hibiya, T., M. Nagasawa, and Y. Niwa (2002), Nonlinear energy transfer within the oceanic internal wave spectrum at mid and high latitudes, *J. Geophys. Res.*, *107*(C11), 3207, doi:10.1029/2001JC001210.

Hosegood, P., and H. van Haren (2006), Sub-inertial modulation of semi-diurnal currents over the continental slope in the Faeroe-Shetland Channel, *Deep Sea Res., Part I*, *53*, 627–655.

MacKinnon, J. A., and K. B. Winters (2005), Subtropical catastrophe: Significant loss of low-mode tidal energy at 28.9°, *Geophys. Res. Lett.*, *32*, L15605, doi:10.1029/2005GL023376.

Millot, C., and M. Crépon (1981), Inertial oscillations on the continental shelf of the Gulf of Lions-Observations and theory, *J. Phys. Oceanogr.*, *11*, 639–657.

Morozov, E. G. (1995), Semidiurnal internal wave global field, *Deep Sea Res., Part I*, *42*, 135–148.

Nagasawa, M., Y. Niwa, and T. Hibiya (2000), Spatial and temporal distribution of the wind-induced internal wave energy available for deep water mixing in the North Pacific, *J. Geophys. Res.*, *105*, 13,933–13,943.

Perkins, H. (1972), Inertial oscillations in the Mediterranean, *Deep Sea Res.*, *19*, 289–296.

Pollard, R. T., and R. C. Millard Jr. (1970), Comparison between observed and simulated wind-generated inertial oscillations, *Deep Sea Res., Part A*, *17*, 813–821.

Reid, J. L., Jr. (1962), Observations of inertial rotation and internal waves, *Deep Sea Res.*, *9*, 283–289.

Siedler, G., and U. Paul (1991), Barotropic and baroclinic tidal currents in the eastern basins of the North Atlantic, *J. Geophys. Res.*, *96*, 22,259–22,271.

Simmons, H. L., R. W. Hallberg, and B. K. Arbic (2004), Internal wave generation in a global baroclinic tide model, *Deep Sea Res., Part II*, *51*, 3043–3068.

van Haren, H. (2004a), Band-width similarity at inertial and tidal frequencies in kinetic energy spectra from the Bay of Biscay, *Deep Sea Res., Part I*, *51*, 637–652.

van Haren, H. (2004b), Spatial variability of deep-ocean motions above an abyssal plain, *J. Geophys. Res.*, *109*, C12014, doi:10.1029/2004JC002558.

van Haren, H. (2005), Tidal and near-inertial peak variations around the diurnal critical latitude, *Geophys. Res. Lett.*, *32*, L23611, doi:10.1029/2005GL024160.

Walter, M., C. Mertens, and M. Rhein (2005), Mixing estimates from a large-scale hydrographic survey in the North Atlantic, *Geophys. Res. Lett.*, *32*, L13605, doi:10.1029/2005GL022471.

Watanabe, M., and T. Hibiya (2002), Global estimates of the wind-induced energy flux to inertial motions in the surface mixed layer, *Geophys. Res. Lett.*, *29*(8), 1239, doi:10.1029/2001GL014422.

Wunsch, C. (1975), Internal tides in the ocean, *Rev. Geophys.*, *13*, 167–182.

Xing, J., and A. M. Davies (2002), Processes influencing the non-linear interaction between inertial oscillations, near inertial internal waves and internal tides, *Geophys. Res. Lett.*, *29*(5), 1067, doi:10.1029/2001GL014199.

H. van Haren, Royal Netherlands Institute for Sea Research (NIOZ), P.O. Box 59, NL-1790 AB Den Burg, Netherlands. (hansvh@nioz.nl)